

Earth's Future

RESEARCH ARTICLE

10.1029/2025EF006648

Key Points:

- The downstream flood risk of 107 hydropower dams around the world was assessed over a period of 40 years
- Forty-one percent of dams studied reduced downstream flood risk while 26% likely worsened it
- Downstream flood risk could be attributed to precipitation intensity, precipitation growth trends, and downstream river length

Supporting Information:

Supporting Information may be found in the online version of this article.

Correspondence to:

F. Hossain,
fhossain@uw.edu

Citation:

Suresh, S., & Hossain, F. (2025). Has hydropower made the world more flood-prone? *Earth's Future*, 13, e2025EF006648. <https://doi.org/10.1029/2025EF006648>

Received 23 MAY 2025
Accepted 20 AUG 2025

Author Contributions:

Conceptualization: Sarath Suresh, Faisal Hossain
Data curation: Sarath Suresh
Formal analysis: Sarath Suresh
Funding acquisition: Faisal Hossain
Investigation: Sarath Suresh, Faisal Hossain
Methodology: Sarath Suresh
Project administration: Faisal Hossain
Software: Sarath Suresh
Supervision: Faisal Hossain
Validation: Sarath Suresh
Visualization: Sarath Suresh
Writing – original draft: Sarath Suresh
Writing – review & editing: Sarath Suresh, Faisal Hossain

© 2025. The Author(s).

This is an open access article under the terms of the [Creative Commons Attribution License](#), which permits use, distribution and reproduction in any medium, provided the original work is properly cited.

Has Hydropower Made the World More Flood-Prone?

Sarath Suresh¹ and Faisal Hossain¹ 

¹Department of Civil and Environmental Engineering, University of Washington, Seattle, WA, USA



Abstract Hydropower has emerged as a cornerstone of global renewable energy initiatives, providing a reliable and renewable source of electricity essential to achieving low emissions targets. However, its expansion, especially in high-precipitation and mountainous regions of developing countries, has sparked growing concerns about its role in exacerbating downstream flood risks. This study critically examines the complex relationship between hydropower development and flood risk through the analysis of 107 major hydropower dams in such regions of the world spanning a period of 40 years. While 41.1% of the studied dams were found to exhibit flood mitigating characteristics by buffering against extreme inflows, 26.2% of dams were likely to exacerbate flood risks, primarily due to a steady increase in precipitation rates and sedimentation-induced capacity loss. Hydropower dams in regions with shorter downstream river lengths were found to be more flood-inducing than flood-protecting. While regions with flood-protecting dams naturally trigger urbanization and economic growth due to perceived safety and stable energy availability, these benefits are accompanied by the cost of increased deforestation. The study identified hotspots in South America and South Asia, where hydropower dams are more likely to be clustered as flood inducing in nature. Overall, the study calls for a paradigm shift in hydropower planning and management, emphasizing the integration of adaptive flood risk mitigation into energy production strategies keeping in mind the anticipated changes in climate and land cover along with a robust sedimentation management strategy during the dam's service lifespan.

Plain Language Summary Hydropower dams have an objective that often competes with flood control. This is particularly the case in developing regions that are mountainous with high precipitation but with insufficient power generation capacity. Given the extensive record of hydropower dam operations we can now build worldwide combined with the fact that more are likely to be built, it is worthwhile to ask if such dams are making the downstream less safe from floods. The findings based on a four-decade long analysis and modeling reveal that the answer is nuanced and that there are many other land and hydrological factors that could help manage current hydropower dams and plan future hydropower dams better using such multi-decadal analysis.

1. Introduction

The development of hydropower has long been championed by some as a sustainable solution to the ever-growing global energy demands in a changing climate. There is a recognition that the world needs to urgently strive toward net zero emission targets to restrain global warming within 1.5°C above pre-industrial levels (IHA, 2022). As part of this urgency, many countries have been actively phasing out non-renewable energy sources like coal, replacing the resulting energy shortfall with renewable options such as hydropower, wind, and solar (Glasgow Climate Pact COP26, 2021). There has been significant growth in the global share of renewable sources of energy over the past two decades, almost doubling from 7.02% of total energy consumed in the year 2000 to 13.69% in 2023 (Energy Institute, 2024).

To meet the ambitious goal of decarbonizing energy production, many argue that an annual global hydropower capacity growth of 2% is necessary (IHA, 2022). In practice, however, this growth has been highly uneven, with the majority occurring in developing regions. For instance, the Organization for Economic Co-operation and Development (OECD) member countries experienced 43.1% total growth in hydropower capacity at an annual growth rate of 0.39% over the last two decades (2000 and 2019). On the other hand, the non-OECD Asian countries increased their capacity by 137.3%, averaging an annual growth rate of 4.42% (IEA, 2021). This trend can be attributed to the mature state of hydropower energy in developed countries, where most viable sites have already been utilized. Consequently, this rapid expansion of hydropower infrastructure in developing countries, which has been ongoing for several decades, coupled with the unique climate and topography of such regions, presents significant challenges.

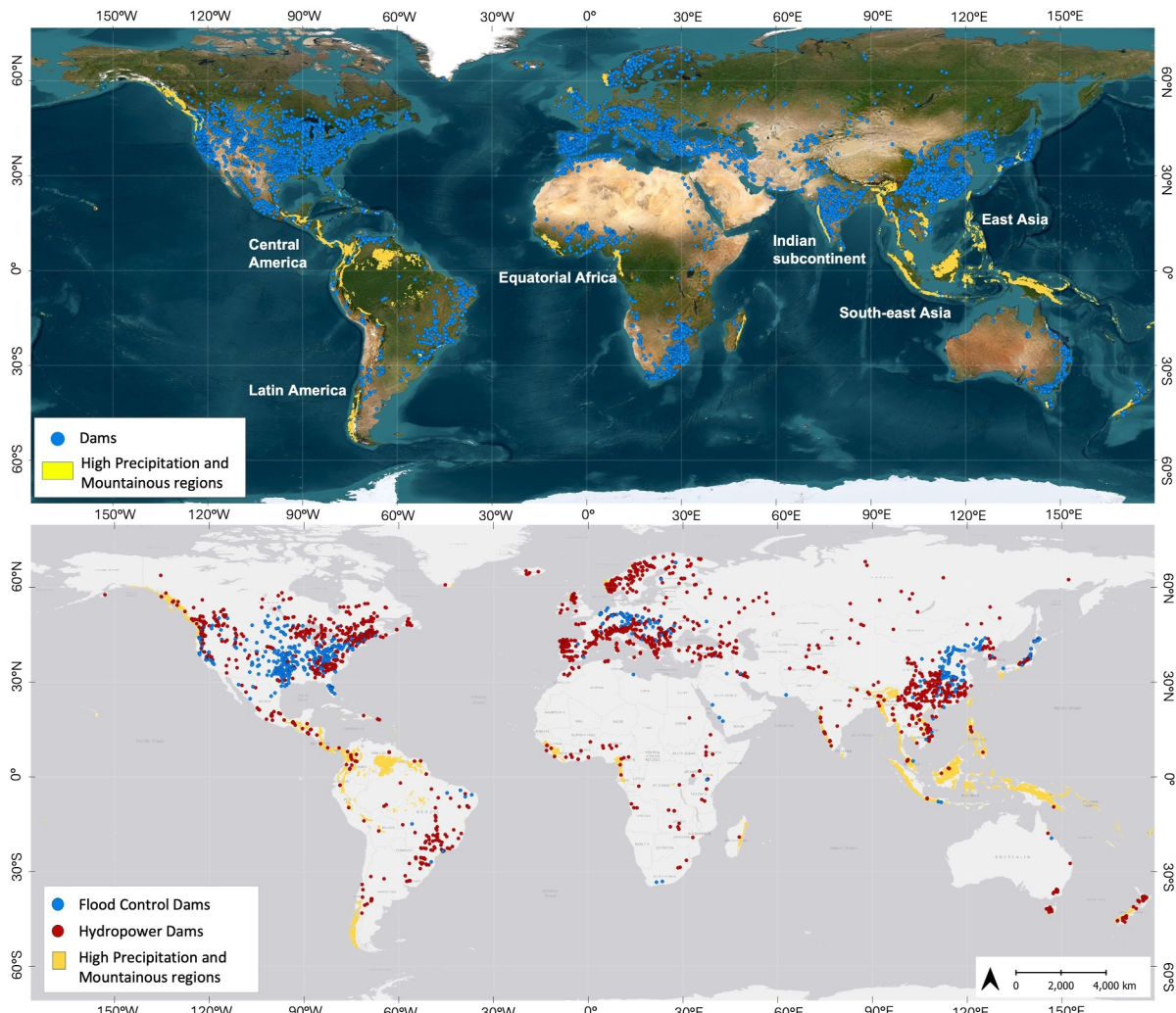


Figure 1. (Top) World map—Regions with high precipitation and mountainous topography shown in yellow where hydropower dams need to provide flood control. Adapted from Figure 1 in Suresh et al. (2024) (Bottom). Location of major dams (GranD database) with designated main use of hydropower generation (marked in red) and flood control (marked in blue). Note that in regions classified as mountainous with high precipitation (highlighted in yellow), hydropower dams dominate. Sources: Dam data—GranD v1.3 (Lehner et al., 2011); Precipitation data—WorldClim v2.1 (Fick & Hijmans, 2017); Mountain data—GMBA Mountain Inventory v2 (Snethlage et al., 2022); Basemaps—ESRI World Imagery, ESRI Light Gray Canvas Map (Esri, DigitalGlobe, GeoEye, i-cubed, USDA FSA, USGS, AEX, Getmapping, Aerogrid, IGN, IGP, swisstopo, DeLorme, HERE, MapmyIndia, and the GIS user community).

Hydropower dams work on the concept of impounding a river's water to maximize the water elevation difference between upstream and downstream locations to convert the potential energy to electricity. This naturally results in increasing the residence time of surface water, leading to higher sedimentation, thermal stratification, less oxygenated water and more methane emissions behind the dams (Lima et al., 2008; Morris & Fan, 1998). While dams and the reservoirs behind them are usually engineered to manage water flow and mitigate flood risks, their construction and operation can disrupt natural hydrological cycles and, paradoxically, exacerbate downstream flood hazards during hydropower operations (Fan et al., 2022; Kumar et al., 2022). This is more likely in regions that are mountainous with high precipitation, where precipitation driven runoffs can cause increased risk of rapid and intense floods, leading to sudden and unexpected high inflows into reservoirs designed to be kept full to maximize energy production. Consequently, an unprepared hydropower reservoir lacking the necessary flood pool to store this unexpected high inflow, can experience disastrous consequences by releasing all the inflow downstream just as suddenly and putting downstream inhabitants at risk without any flood preparedness (Suresh et al., 2024).

As seen in Figure 1, approximately 90% of such already flood-prone, high precipitation and mountainous regions lie in the developing regions of the world, such as South and Southeast Asia, Central and South America, and West African countries.

Due to increasing irregularity and variation in precipitation trends and associated runoffs (Willis et al., 2011), conventional reservoir operations based on pre-dam hydroclimatic data are proving ineffective in providing sufficient flood cushioning. In recent years, many flooding events have been reported where the failure to adjust reservoir levels in a timely manner was considered a root cause (Kundu & Mothikumar, 1995; Zhang et al., 2014).

A notable example is the 2018 floods in Kerala, India, which claimed more than 400 lives, and caused damage in excess of 5 billion US dollars (Pramanick et al., 2022). The flooding was primarily attributed to intense precipitation driven by a propagating low-pressure weather system from the Bay of Bengal which overlapped with the ongoing Monsoon precipitation system from the Indian Ocean (Sudheer et al., 2019). Most reservoirs in the region were already at or near maximum capacity prior to the peak precipitation event leading to complete loss of flood moderation capabilities (Suresh et al., 2024). Another case of dam operations negatively affecting downstream flooding was seen in the 2011 Thailand Mega flood, that killed more than 800 people, due to a record high precipitation event (Gale & Saunders, 2013). The weakness of existing operations of major hydropower dams such as Bhumibol and Sirikit dams, due to rigid reservoir operations was considered one of the main reasons (Loc et al., 2023; Poaponsakorn et al., 2014). Similarly, the Volta River in Ghana, which has witnessed multiple flooding across the years due to unexpected releases from the Bagre hydropower dam in Burkina Faso (Abass et al., 2022), is another example of floods caused by hydropower reservoir operations. In this case, lack of transboundary cooperation and timely sharing of reservoir operations data only exacerbated the flood management downstream in Ghana. A similar case in point is in the upper Indus basin between India (upstream) and Pakistan (downstream) where the downstream Mangla Dam of Pakistan on the Jhelum River is often forced to spill large amounts of water due to unexpected transboundary release from India.

As seen from these historical events, hydropower reservoirs that are not adequately prepared for sudden inflows can lead to catastrophic flooding, causing loss of life, economic damage, and environmental degradation. It is therefore crucial that an examination of the past be conducted to assess the flooding risk that is attributable to the rapid growth of hydropower in these regions. Since more than one-third of the global population lives within 50 km of major hydropower dams (Fan et al., 2022), understanding the dynamics between hydropower expansion and flood risks is crucial not only for planning future hydropower projects but also for policy making to protect downstream communities from potential flood hazards and catastrophic loss of life.

This study aims to critically examine the intersection of hydropower growth and flood risk to comprehensively answer the question with extensive data and methods—“*Has hydropower made the world more flood-prone?*” The findings will help answer broader questions on whether adjustments are required for either operations of current hydropower dams or planning of future hydropower dams to mitigate future downstream flood risks.

The paper is organized as follows: The remainder of this section provides a brief description of the study area. Section 2 showcases the data sets used. Section 3 outlines the key concepts and methodology employed. Section 4 discusses the results, examining qualitatively and statistically, the links between hydropower dams, flood risks, and other factors. Finally, Section 5 summarizes the key findings, limitations, and outlines future research directions.

1.1. Study Sites

One hundred and seven major hydropower dams located in high precipitation and mountainous regions were chosen as the study sites (Figure 2). We arrived at this set of hydropower dams based on an exhaustive search of 7,000+ large dams in the GranD v1.3 data set (Lehner et al., 2011) and filtering it with topography and hydroclimate to obtain those located in regions with steep topography and high precipitation. High precipitation zones were defined using a data-driven threshold approach applied to long-term mean annual precipitation data from the WorldClim version 2 data set (Fick & Hijmans, 2017). Specifically, regions falling within the top 5th percentile of global land-surface precipitation values (approximately $\geq 1,900 \text{ mm/year}$) were classified as high-precipitation zones. This percentile-based method allows for a globally consistent and objective delineation of high precipitation regions, consistent with standard practices in hydrologic and climate impact assessments (Alexander et al., 2006; Milly et al., 2002).

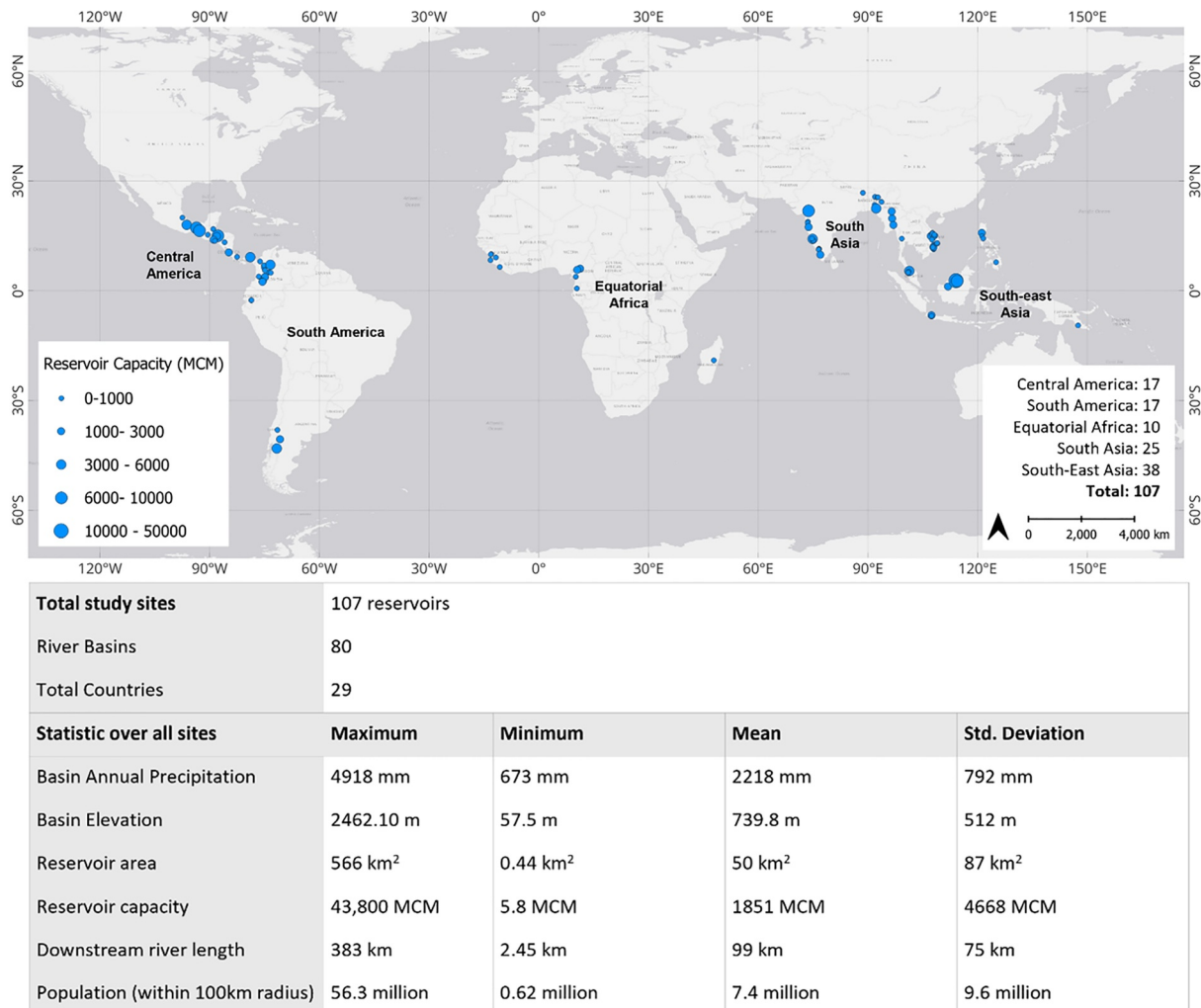


Figure 2. (Top) Location of 107 hydropower dams chosen as the study sites. The size of the marker indicates the capacity of the reservoir in MCM. Region-wise split of the study sites is shown in the bottom right. (Bottom) Study site general statistics. See Table S1 in Supporting Information S1 for individual study site details. MCM stands for Million Cubic Meter. Sources: Dam data—GranD v1.3 (Lehner et al., 2011); Basemap—ESRI Light Gray Canvas Map (Esri, DeLorme, HERE, MapmyIndia).

Mountainous areas were delineated using the Global Mountain Biodiversity Assessment (GMBA) mountain inventory data set, which classifies terrain based on a combination of elevation and ruggedness metrics. The final study area was defined as the intersection of high precipitation zones and GMBA-defined mountain regions. This mask was then overlaid with the dam database, and only dams located within these intersecting zones were retained. Dams in high-income countries within this mask, such as those in Norway, Japan, or the Pacific Northwest (US), were excluded to maintain the focus on developing regions.

Hydropower dams where floods are generally rare (such as in arid, semi-arid regions) or where the existing hydrology is not conducive to flood generation were also ignored. Such dams are unlikely to exacerbate downstream flood risk due to operations unless there is a structural failure. Furthermore, to answer the question of the study, we required a statistically significant sample of hydropower dams spread over diverse climate, geography and socio-economic contexts (see Table 1).

2. Data

A study of this nature spanning the globe where in situ data are generally scarce, requires full utilization of satellite remote sensing and Earth observation (EO) data that now has a record longer than 40 years (Durand

Table 1
Key Data Sets

Data	Type	Resolution	Time period used	Source
Landsat (4, 5, 7, 8)	Satellite-Optical	30 m, 16 days interval	1986–Present	Microsoft planetary computer: Landsat collection 2 level 2
SRTM DEM	C, X-band SAR	30 m, Vertical accuracy: ± 10 m	2000	Google Earth engine data catalog: NASA SRTM digital elevation 30 m
ERA 5-Precipitation	Climate reanalysis	0.25° (~ 31 km) (Hourly/ Monthly)	1986–Present	Copernicus climate data store: ERA5 for precipitation and climate data
GranD	Reservoir database	Global reservoir data	Version 1.3 (2011 update)	Global reservoir and dam database (GranD)
HydroRivers/ HydroBasins	River network/Basin data	Global	Current	HydroSHEDS: WWF-HydroRivers (Lehner & Grille, 2013)
GlobPop	Population data	Gridded population data	2000–Present	WorldPop/Global Human Settlement Layer (GHS)
ESA climate change initiative	Land cover map	300 m	1992–Present	ESA climate change initiative: Land cover map
DMSP, VIIRS	Nightlight data	30 arc-s (~ 1 km)	1992–2021	Harmonized global night time lights
NOAA NCEP	Temperature (Min and Max) /Wind speed	0.0625° (~ 7 km)	1985–Present	NOAA NCEP/Climate prediction centre

et al., 2021). Satellite data can offer a wide range of valuable information and insights on hydrological changes, land use, and reservoir operations (Sheffield et al., 2018). The Landsat series from the National Aeronautics and Space Administration (NASA) and the Sentinel constellation from the European Space Agency (ESA) provide comprehensive data on surface water features. By combining water level estimates with remotely sensed surface area data, it is possible to estimate changes in reservoir storage (Chen et al., 2022; Cooley et al., 2021; Gao, 2015). These variations, along with hydrological model-based inflow data, enable the calculation of reservoir releases through the use of water balance equations (Bonnema & Hossain, 2017, 2019; Minocha et al., 2024; Zhong et al., 2020).

Climate data from ERA5, a global atmospheric reanalysis product provided by the European Centre for Medium-Range Weather Forecasts (ECMWF), and NOAA NCEP (National Centers for Environmental Prediction), were used as sources for long-term, high-resolution record of precipitation, temperature and wind speed. Together, these data sets allow for the reconstruction of historical inflows, reservoir evaporation rates, and precipitation variability, forming a solid foundation for understanding long-term climate impacts on reservoir operations.

Additional data sets used were on population (Liu et al., 2024), land cover, and nighttime light radiance from sources such as the Global Human Settlement Layer (GHS), the ESA Climate Change Initiative Land Cover (CCI) maps, and VIIRS/DMSP nighttime light data (Li et al., 2020) provide vital socio-economic and land-use information. Nighttime light data serves as a proxy for human activity and energy demand, while population grids enable assessments of demographic changes and urban expansion in proximity to hydropower reservoirs. Land cover maps deliver detailed annual updates, allowing for the monitoring of forest cover loss, urbanization trends, and agricultural expansion upstream and downstream of reservoirs.

3. Methods

We used satellite data and hydrological model-based framework to generate reservoir inflows, storage patterns, releases, and extents in downstream flood. The primary tool employed was the Reservoir Assessment Tool (RAT 3.0), originally described by Minocha et al. (2024). As part of this study, the RAT 3.0 framework was modified to incorporate nearly 40 years of Landsat surface water area data and ERA5 reanalysis-based meteorological forcing, enabling long-term retrospective reservoir analysis. The tool is used in conjunction with other satellite data-based workflows to assess the downstream flood risk for hydropower dams in the study regions, and to examine any relations with changing climate patterns and urbanization. The overall framework of the study is presented in Figure 3, containing the following key components: Study site selection and data collection; Initial flood risk assessment; Confirmatory testing; Analysis of results.

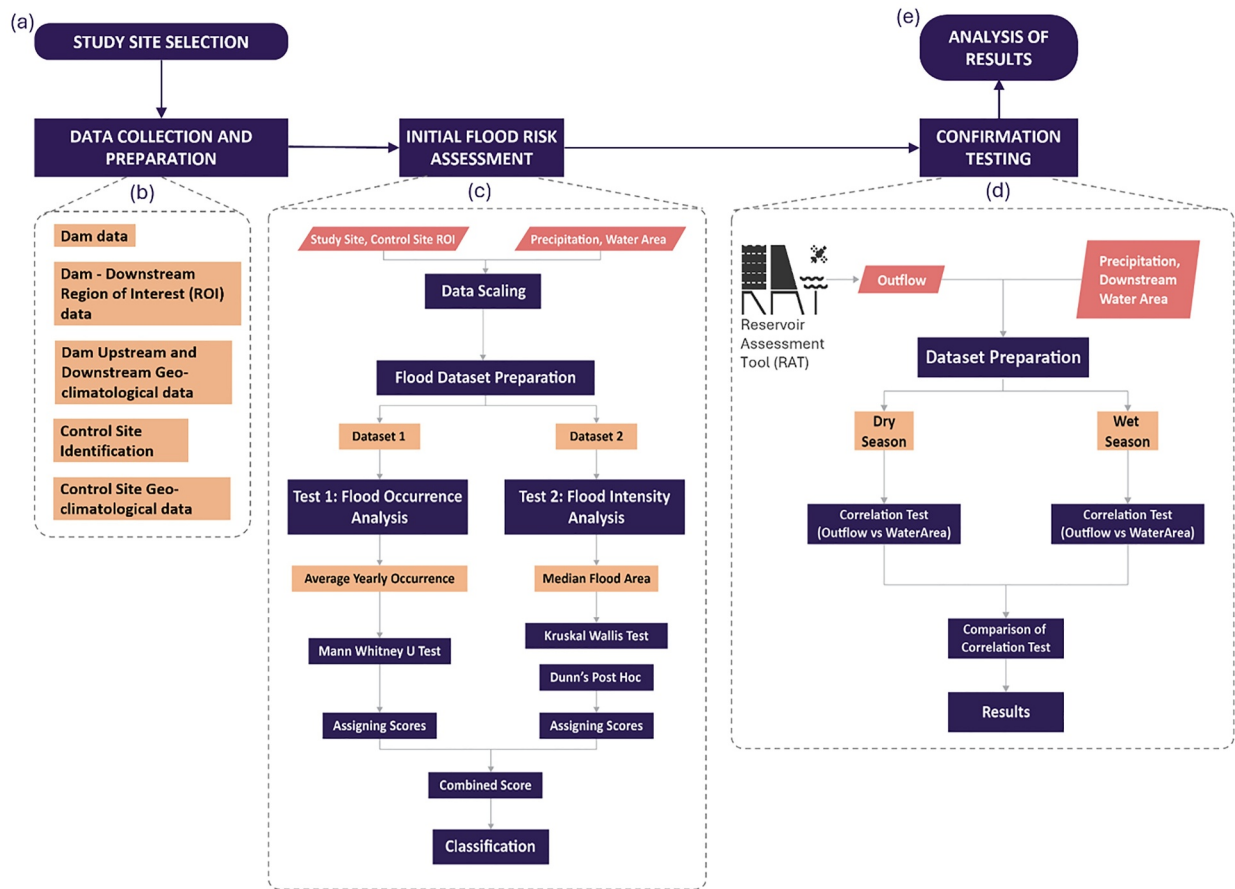


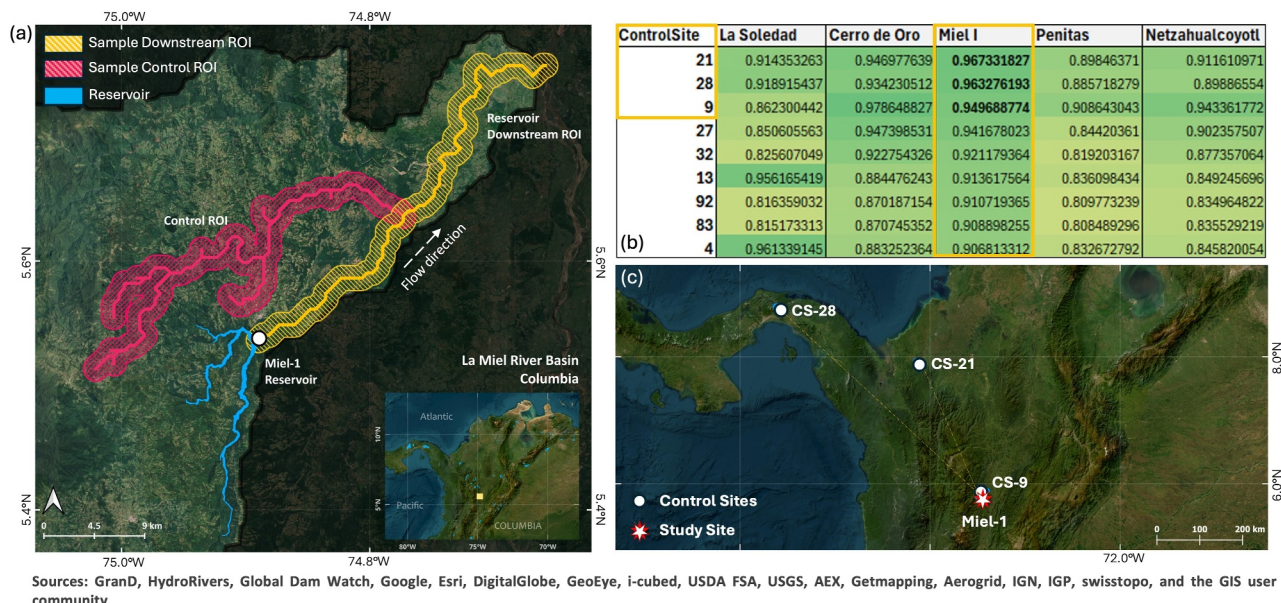
Figure 3. Overarching methodology to assess flood risk of hydropower dams with detailed methodology of components. The workflow is organized into five key components: (a) Study site selection, (b) Data collection and preparation, (c) Initial flood risk assessment, (d) Confirmation testing, and (e) Analysis of results. The flowchart presents detailed sub-methodologies for components (c) and (d).

3.1. Initial Flood Risk Assessment

An intuitive assessment of the impact of hydropower dams on downstream flood risk should involve analysis of flood extents of the same region of interest (ROI) under pre-dam and post-dam conditions. However, due to the considerable age of most dams in the world (constructed before the satellite era of 1980s), there is little or no satellite data from the pre-dam era. To overcome this issue, we used the concept of “control” sites, defined as similar hydroclimatic and geographically close regions free from the influence of dams. These control sites provided a comparative baseline for carrying out “control” versus “experiment” (i.e., hydropower dams) comparisons. By comparing these control sites with regions influenced by hydropower dams (the experiment), it is possible to infer in the preliminary sense, the effects of hydropower dam operation on downstream flooding risks. As an example, Figure 4a shows a side-by-side comparison of a control site ROI and a reservoir downstream ROI, located in the Magdalena River basin in Colombia. Suitable control sites were identified for each dam study site. The precipitation and water area time series were statistically compared to judge the role played by hydropower dams in worsening or protecting its downstream area from high precipitation induced floods.

3.1.1. Control Site Selection

A total of 95 control sites, free of influence of upstream dams were carefully identified. These control regions are areas that contain significant river networks but do not contain any kind of stored surface water features such as lakes or reservoirs. For each “experiment” study site, analysis of flood risk was conducted against three control sites.



Sources: GranD, HydroRivers, Global Dam Watch, Google, Esri, DigitalGlobe, GeoEye, i-cubed, USDA FSA, USGS, AEX, Getmapping, Aerogrid, IGN, IGP, swisstopo, and the GIS user community

Figure 4. (a) Example of a control site region of interest (ROI) (shown in red) and a downstream ROI (shown in yellow) of the Miel-1 reservoir (shown in blue) located in the La Miel River Basin, Colombia. The control site ROI is free from the influence of any type of upstream reservoirs. (b) Study sites and similarity scores of control sites. Similarity scores of top 3 control sites for Miel-1 are highlighted in red. (c) Location of top 3 control sites for Miel-1 study site. Basemap Source: ESRI World Imagery—Esri, DigitalGlobe, GeoEye, i-cubed, USDA FSA, USGS, AEX, Getmapping, Aerogrid, IGN, IGP, swisstopo, DeLorme, HERE, MapmyIndia, and the GIS user community.

As individual study site river basins can be small or lack undammed tributaries, it is not always feasible to locate appropriate controls within the same basin. Thus, the selection of three nearby control sites was based on the computation of a similarity score, which quantifies the degree of similarity between a control site's ROI and that of the corresponding study site.

For both study and control sites, the ROI was defined as a 20 km buffer on either side of the mainstem river channel. This buffer distance was chosen as a reasonable approximation of the flood-prone zone surrounding a river segment. It also provides a standardized unit of analysis, enabling consistent comparison across a wide range of geographic and hydrologic settings. Due to the steep and mountainous terrain of the study sites, narrow and incised reaches immediately downstream of the dam rarely inundate. Thus, their downstream ROI's were extended till the river entered a low-slope floodplain and interacted with a terminal water body outlet such as a sea or lake, where flood signatures can be meaningfully detected.

For a given study site, similarity scores are then computed between the study site ROI and each of the 95 control sites ROI's based on weighted parameters such as average precipitation, average slope, cartesian distance, and percentage of urban land cover, as expressed in Equation 1. The method for computing precipitation differs between study and control sites to reflect their distinct hydrological configurations. For study sites, precipitation was aggregated over the entire upstream catchment, since it directly influences reservoir inflows and operational behavior. For control sites, which do not contain any upstream storage features such as reservoirs or lakes, precipitation was computed across the full control ROI. These ROIs are selected to span from the headwaters of their own local catchments to flatter downstream terrain, mirroring the spatial coverage of study site ROIs. The analysis focuses on the temporal characteristics of precipitation, particularly the timing and recurrence of extreme events, rather than the absolute magnitude of rainfall. High precipitation peaks, which are the primary drivers of flood signals, are reliably detected even when averaged across the ROI. The variables were normalized using min–max scaling, with minimum and maximum values calculated from the full set of 95 control sites per study site. This ensured that each score reflected a context-specific and internally consistent comparison, with resulting similarity scores ranging from 0 to 1. The sorted similarity scores are then used to identify the three most similar control sites for each study site.

$$\text{Similarity score}(S) = w_p \cdot \text{PrecipitationScore} + w_d \cdot \text{DistanceScore} + w_s \cdot \text{SlopeScore} + w_u \cdot \text{UrbanisationScore}$$

$$S = w_p \cdot \left(1 - \frac{|P_{\text{study}} - P_{\text{control}}|}{P_{\max} - P_{\min}}\right) + w_d \cdot \left(1 - \frac{D_{\text{study,control}}}{D_{\max}}\right) + w_s \cdot \left(1 - \frac{|S_{\text{study}} - S_{\text{control}}|}{S_{\max} - S_{\min}}\right) + w_u \cdot \left(1 - \frac{|U_{\text{study}} - U_{\text{control}}|}{U_{\max} - U_{\min}}\right) \quad (1)$$

Here, the weights w_p , w_d , w_s , and w_u were assigned the values of 0.5, 0.2, 0.2, 0.1, respectively. The weights were chosen in such a way that the three most similar control sites for every dam study site had a similarity score of at least 0.8. Although study-site ROIs can extend further downstream than their matched controls, including average slope in Equation 1 ensures that both study and control ROIs encompass comparable low-slope flood-prone reaches, thereby minimizing any bias that raw reach-length differences might introduce. The choice to weigh precipitation more heavily reflects its critical role in flood generation processes. However, during sensitivity checks, it was observed that increasing the precipitation weight further (e.g., to 0.6) could lead to the selection of climatologically similar but geographically distant control sites. To balance hydrological relevance with spatial comparability, particularly considering regional water management practices, the final weight combination was chosen. Figures 4b and 4c shows the computed similarity scores of control regions for a sample study site, and their locations.

3.1.2. Data Collection and Scaling

For both the study site and control site ROI's, the surface area module of RAT 3.0 was modified to compute the water area extent utilizing over 40 years of Landsat data at a spatial resolution of 30 m and a temporal resolution of 16 days. Water pixels were identified using the Modified Normalized Difference Water Index (MNDWI) spectral index, and binary water masks were extracted using the Otsu method of automated thresholding (Otsu, 1979), which determines an optimal threshold based on the distribution of MNDWI values. Cloud correction is carried out utilizing the JRC Global Surface Water data set (Pekel et al., 2016), following the Zhao and Gao (2018) method. Readers are referred to Suresh et al., 2024 for a more detailed explanation of the water area extraction technique.

Critically, the water area extent for each ROI is computed as the area of the total number of MNDWI-classified water pixels. The water area extent data and gridded precipitation data obtained from the ERA 5 Reanalysis product are then independently min–max normalized to their own 40-year historical ranges (1984–2023). This scales all data points to a common range of 0–1 and ensures that the water area is scale-invariant and avoids the bias that per-length or per-area measures would introduce when ROI's differ in sizes.

3.1.3. Flood Occurrence Frequency Analysis (Test 1)

Employing statistical tests ensured a robust and scalable method for evaluating flood risk across numerous study sites. The first test assessed flood risk by comparing the frequency of large surface water inundation events during high precipitation periods between the study site and its control sites. The 40-year normalized water area and precipitation data were utilized to generate a Flood Event Data set, containing the counts of instances where both the precipitation and water areas were greater than 90th percentiles simultaneously. Annual flood frequencies were computed by grouping flood event data by year, and the average annual frequency was used for comparison.

If the study site exhibited the highest or lowest average flood frequency, it was preliminarily classified as likely flood inducing or likely flood protecting, respectively, and flagged for further confirmatory testing (Figure 3d). The Mann-Whitney *U* Test (Mann & Whitney, 1947) was employed to compare flood frequencies between the study site and the second-ranked control sites. Since the data sets employed contain high percentile values, it is non-normally distributed. Thus, typical tests such as Analysis of Variance (ANOVA), or Student's *t*-test are not applicable. If the *p*-value from the tests is less than 5%, the null hypothesis (no significant difference between the study site and the control) is rejected, indicating a statistically significant difference.

3.1.4. Flood Intensity Analysis (Test 2)

To further assess the flood risk, a second test was performed to compare the magnitude of flooding (intensity) across sites. A precipitation response data set was created by extracting normalized water area values during instances

where precipitation exceeded the 90th percentile. The median flood intensity was then computed for the study site and its three control sites. If the study site had the lowest or highest median flood intensity, then it is indicative of a “Likely Flood Protecting” or “Likely Flood Inducing” nature, respectively for the hydropower dam.

The Kruskal-Wallis test (Kruskal & Wallis, 1952), an extension of the Mann-Whitney *U* Test, is used to compare the medians of the study site with the three controls. If the *p*-value of the test is less than 0.05, it indicates that at least one group median is significantly different from the others. The Dunn's Post-hoc test (Dunn, 1964) is subsequently employed to identify specific groups with significant differences and Bonferroni Correction is applied to control for Type I error (false positives). This helps confirm whether the study site is statistically different from the control site. The post-hoc tests with the correction applied returns an adjusted *p*-value matrix for all study site and control site combinations. If the maximum *p*-value thus obtained for any of the study site-control site combination is less than 5%, then the result is considered to be statistically significant.

3.1.5. Scoring and Classification

Based on the results of the various statistical tests, scores are assigned for Tests 1 and 2. The specifics of criteria for Test 1 and 2 scores are explained in Table S2 in Supporting Information S1. A combined score is then generated as the sum of the Test 1 and Test 2 scores. This score has a range of 2–10, with a score of 2 showing high confidence of likely flood inducing behavior and a score of 10 indicating high confidence of likely flood protecting nature. The scoring categories are as follows:

- Sum of 2: Likely Flood Inducing hydropower dam (high confidence)
- Sum of 3–5: Likely Flood Inducing hydropower dam (moderate confidence)
- Sum of 6: Ambiguous
- Sum of 7–9: Likely Flood Protecting hydropower dam (moderate confidence)
- Sum of 10: Likely Flood Protecting hydropower dam (high confidence)

For illustration purposes, Figure 5 shows quantitatively the values obtained for a sample study site of Avalanche, located in the Cauvery River basin, India. It was classified as “Likely Flood Protecting” (moderate confidence).

3.2. Confirmatory Testing

For the dams classified as “Likely Flood Inducing” with either high or moderate level of confidence, another round of testing was employed, where the reservoir outflow is checked against downstream flood area time series.

As illustrated in Figure 3d, the final stage of testing focuses on evaluating the correlation between upstream reservoir outflows and downstream flood areas across both wet and dry seasons. This analysis determined the extent of dam's direct influence on downstream flooding. If a dam exhibits a higher correlation between reservoir outflow and downstream flood area during the wet season compared to the dry season, it provides strong evidence that the dam's operations are likely exacerbating downstream flooding. Such sites are then classified as “Likely Flood Inducing” with a high degree of confidence. The subsequent sections provide a further explanation on the outflow computation, data set preparation, and correlation analysis.

3.2.1. Outflow Computation

The Reservoir Assessment Tool (RAT 3.0) (Minocha et al., 2024) was utilized to compute the reservoir outflow for all sites classified as “Likely Flood Inducing” using data generated reservoir outflow over more than 30 years. For a given reservoir, RAT solves a simple mass balance (Figure 6) that uses inflow, storage change, and evaporation data to compute outflow.

Inflow is modeled using the semi-distributed, gridded macro scale hydrological model, VIC 5.0 (Hamman et al., 2018), which utilizes meteorological forcing data from ERA 5 and NOAA NCEP, converted via MetSim (Bennet et al., 2020), and routes runoff into streamflow data with the VIC Routing Model (Lohmann et al., 1998) to determine reservoir inflows. Reservoir surface area time series is derived from Landsat satellite data, corrected for cloud cover using historical water occurrence probabilities (Pekel et al., 2016) and smoothed with weighted cloud cover adjustments (Zhao & Gao, 2018). Evaporation, computed using the Penman equation (Penman, 1948), is the primary water loss factor, while area-elevation relationships are established using SRTM DEM data, fitted to a power law curve from the reservoir's full level to its base. RAT has a temporal resolution of

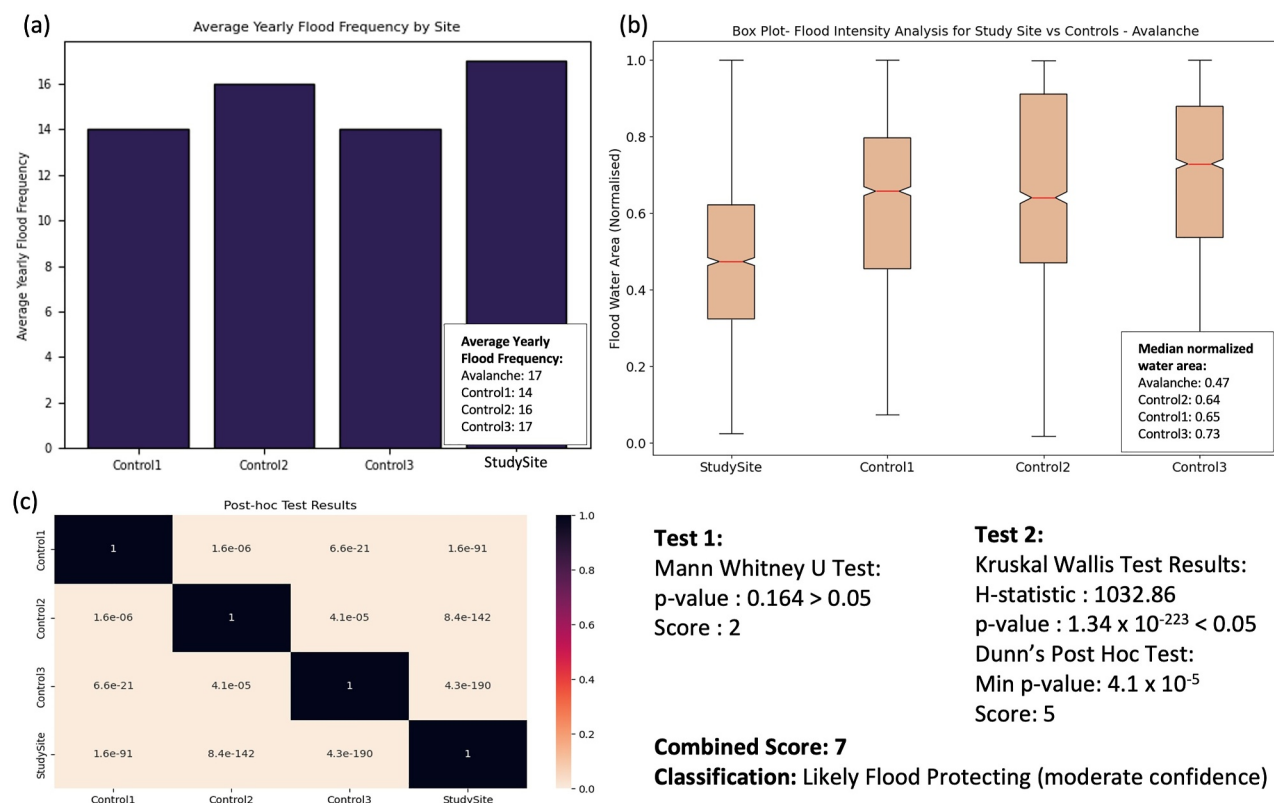


Figure 5. (a) Test 1—Average yearly flood occurrence values for sample study site of Avalanche, India versus controls. (b) Test 2—Box plot showing distribution of flood water area of study site versus controls. (c) Test 2—*p*-value result matrix of Dunn's post-hoc test. Numerical values of the statistical tests, individual and combined test scores, and classification are provided in the bottom right section.

1 day for inflows and 2–5 days for surface area, storage change, and outflow estimates (Biswas et al., 2021; Das et al., 2022; Minocha et al., 2024). Reservoir modeling was carried out for a period of 35 years (1988–2023) with 2 years of initial data used for spin-up of the hydrological model. Figure S2 in Supporting Information S1 showcases data generated by RAT for a sample reservoir.

RAT3.0 has undergone extensive validation across a range of geographic and hydrologic contexts. Prior studies have shown that RAT can reproduce observed outflows with good accuracy. In the Mekong Basin, it achieved a correlation of up to 0.55 and a relative RMSE of 11.3% (Das et al., 2022). In Kerala, India, RAT3.0 obtained correlation reached up to 0.88 with a relative RMSE of 3.9% (Suresh et al., 2024). For Hidkal Dam, India, RAT captured the timing of flow rise and recession accurately (Minocha, Das, & Hossain, 2025). An earlier mass-balance implementation of a more primitive version of RAT also achieved a Nash-Sutcliffe Efficiency (NSE) of 0.30 and annual relative RMSE of 20.4% for Kaptai Dam, Bangladesh (Bonnema et al., 2016). RAT has additionally been validated in terms of storage change across 80+ reservoirs with $R^2 > 0.8$ in most cases (Biswas et al., 2021), and VIC-derived inflows have been benchmarked against in situ discharge records in 25 river basins (Ahmad & Hossain, 2020). RAT has also been further augmented by incorporating regulated inflow from upstream reservoirs to improve inflow estimates (Das, Hossain, et al., 2024). While outflow magnitudes may contain some bias due to uncertainties in inflow or area-elevation relationships, RAT has consistently captured the timing and pattern of reservoir release events, particularly during floods.

Readers are encouraged to refer to Suresh et al. (2024) for further specifics and information on optimizing RAT3.0 for high precipitation mountainous catchments.

3.2.2. Data Set Preparation and Correlation Tests

Precipitation, downstream inundated water area, and reservoir outflow data were analyzed by categorizing them into wet and dry seasons. The seasons were determined by applying K-Means clustering to the mean monthly

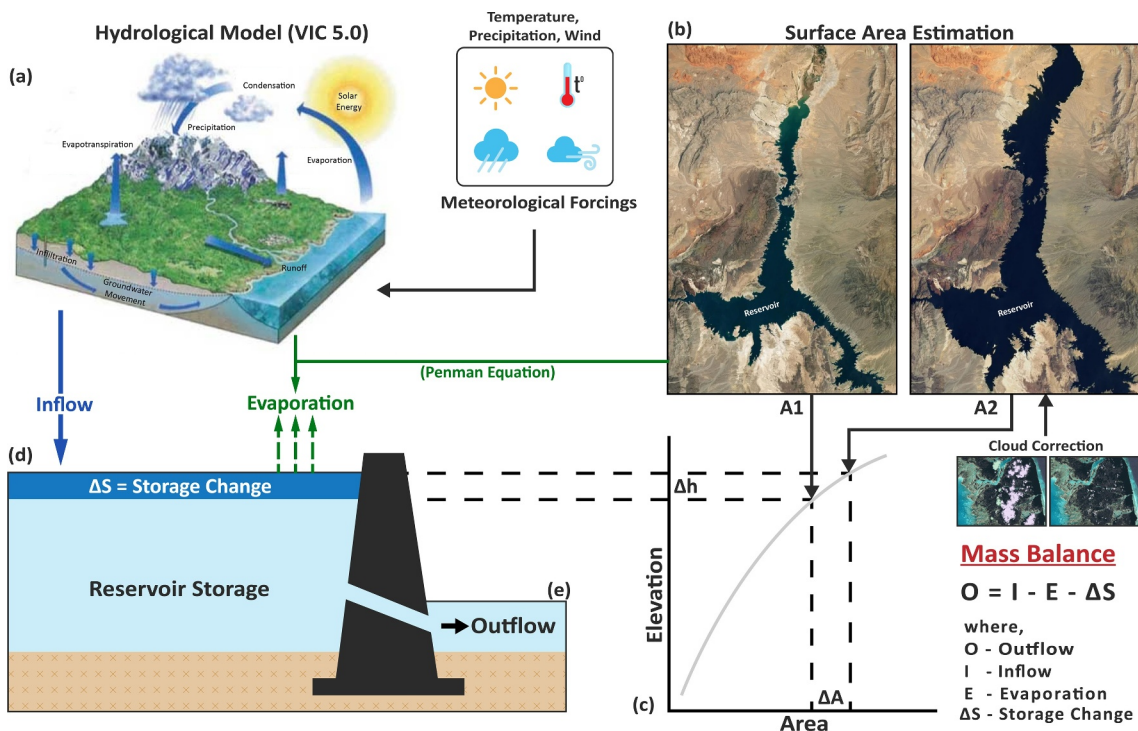


Figure 6. Components of Reservoir Assessment Tool 3.0. (a) Hydrological model (VIC 5.0), (b) surface area estimation (Inset images obtained from Landsat 8 satellite imagery over Lake Mead, California). (c) SRTM derived area elevation curve, (d) evaporation and change in storage, (e) outflow (Minocha et al., 2024). Reproduced from Figure 4 in Suresh et al., 2024.

precipitation values, resulting in two distinct groups. Figure S3 in Supporting Information S1 illustrates the precipitation-based identification of wet and dry seasons.

For each season, the reservoir outflow values corresponding to the highest downstream water area were identified. The relationship between reservoir outflow and downstream water area was quantified using the Spearman correlation coefficient for the wet and dry season data sets. Spearman correlation was selected over Pearson correlation due to the non-normal distribution of the outflow and water area data sets. Additionally, Spearman correlation is less sensitive to outliers.

Reservoirs were confirmed as “Likely Flood Inducing” with a high degree of confidence if the following conditions were met:

- The Spearman correlation between the downstream water area and reservoir outflow during the wet season was positive.
- The correlation coefficient for the wet season exceeded that of the dry season.
- The difference in correlation coefficients between the wet and dry seasons was greater than 0.2.

Reservoirs meeting these criteria exhibited a stronger association between outflows and downstream water areas during high-precipitation periods. This indicated that reservoir operations during the wet season contributed to elevated downstream inundated water areas, potentially increasing flood risks. The remaining sites, with both moderate and high confidence initial classification, that do not meet the confirmatory criteria, are then reclassified as simply “Likely Flood Inducing.” At this point, dams with flood protecting nature are also labeled as “Likely Flood Protecting” irrespective of their initial level of confidence.

4. Results

In the first phase of testing, all 107 hydropower dam study sites were compared with respect to 3 control sites as explained earlier in Section 3.1. The results of flood intensity analysis and flood frequency analysis are shown in Figures 7a and 7b. The distribution of the classification indicates that the majority of the study sites are Likely

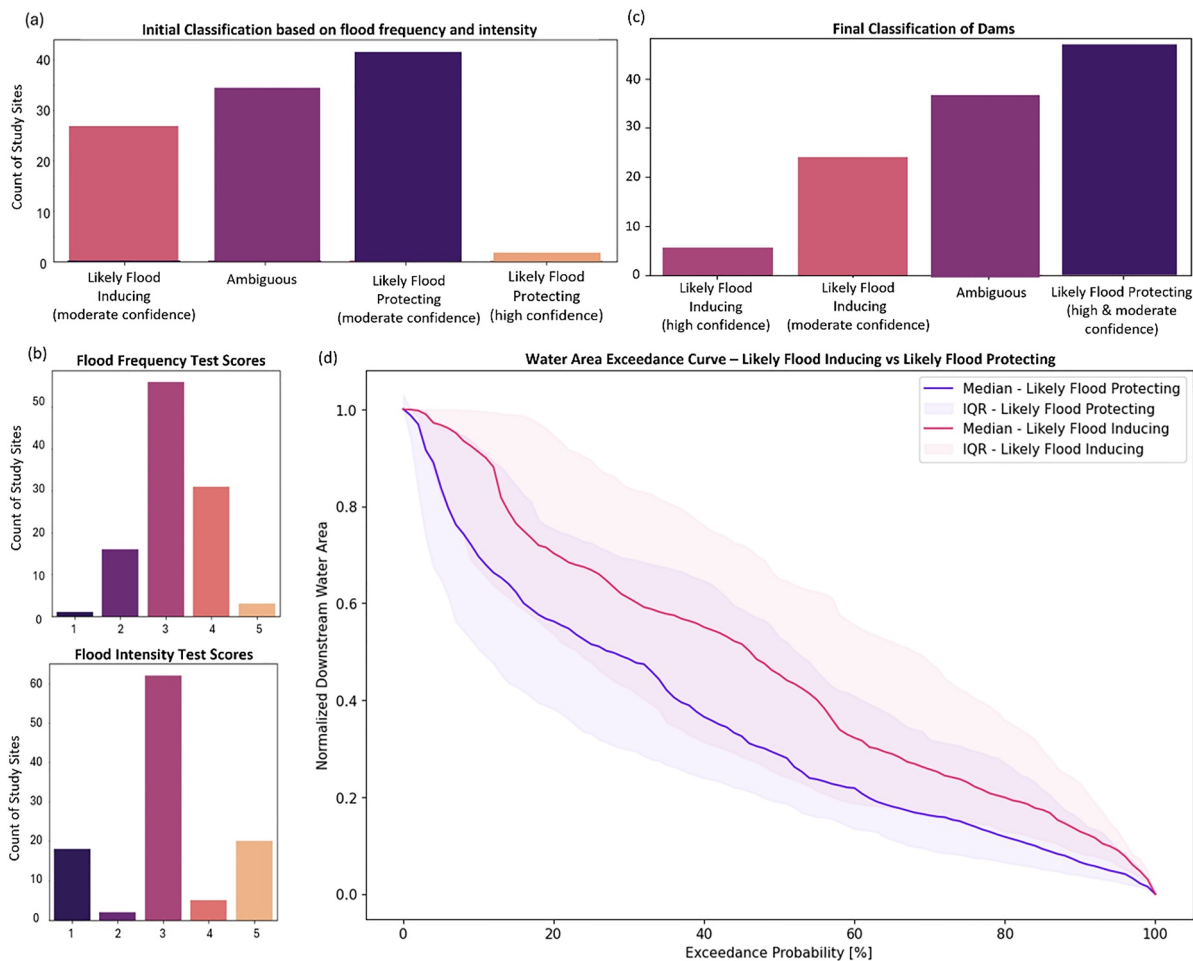


Figure 7. (a) and (b) Initial flood risk assessment results. (a) Number of study sites with specific scores for Test 1 and Test 2. (b) Number of study sites with specific initial classification labels. (c) Confirmatory Analysis—Number of study sites with final classification labels. (d) Water area exceedance curves for all study sites classified as “Likely Flood Inducing” and “Likely Flood Protecting.” The shaded regions represent the interquartile range (IQR)—values between 25th and 75th percentiles, that indicates the variability.

Flood Protecting in nature (41.1%) with a moderate or high level of confidence. Test 1, Test 2, and combined scores for all study sites are shown in Figure S4 in Supporting Information S1.

The water area exceedance curves for study sites classified as “Likely Flood Inducing” and “Likely Flood Protecting” are illustrated in Figure 7d. These curves provide a comparative analysis of normalized downstream water area distributions for the two classifications, shedding light on the duration and magnitude of water areas across different exceedance probabilities and therefore return periods. The median curves reveal clear differences, with flood-inducing hydropower dam sites consistently exhibiting larger normalized downstream water areas compared to flood-protecting sites across all exceedance probabilities. The picture that emerges is that during extreme events associated with long return periods, sites classified as “Likely Flood Inducing” are significantly more prone to extensive inundation, highlighting their heightened vulnerability to severe flooding (discussed in more detail in Section 5).

In the second phase of confirmatory testing, those sites that were initially classified as “Likely Flood Inducing” were explored further. The relationship between downstream water area and RAT3.0-based reservoir outflows was evaluated separately for wet and dry precipitation periods to assess the influence of reservoir operations on the downstream region. Since the downstream water area is also significantly influenced by natural runoff, high correlations between reservoir outflow and inundated water area were not expected. Subsequently, Spearman correlation values were generally low across most sites. Only seven study sites (6% of the total sites) showed a

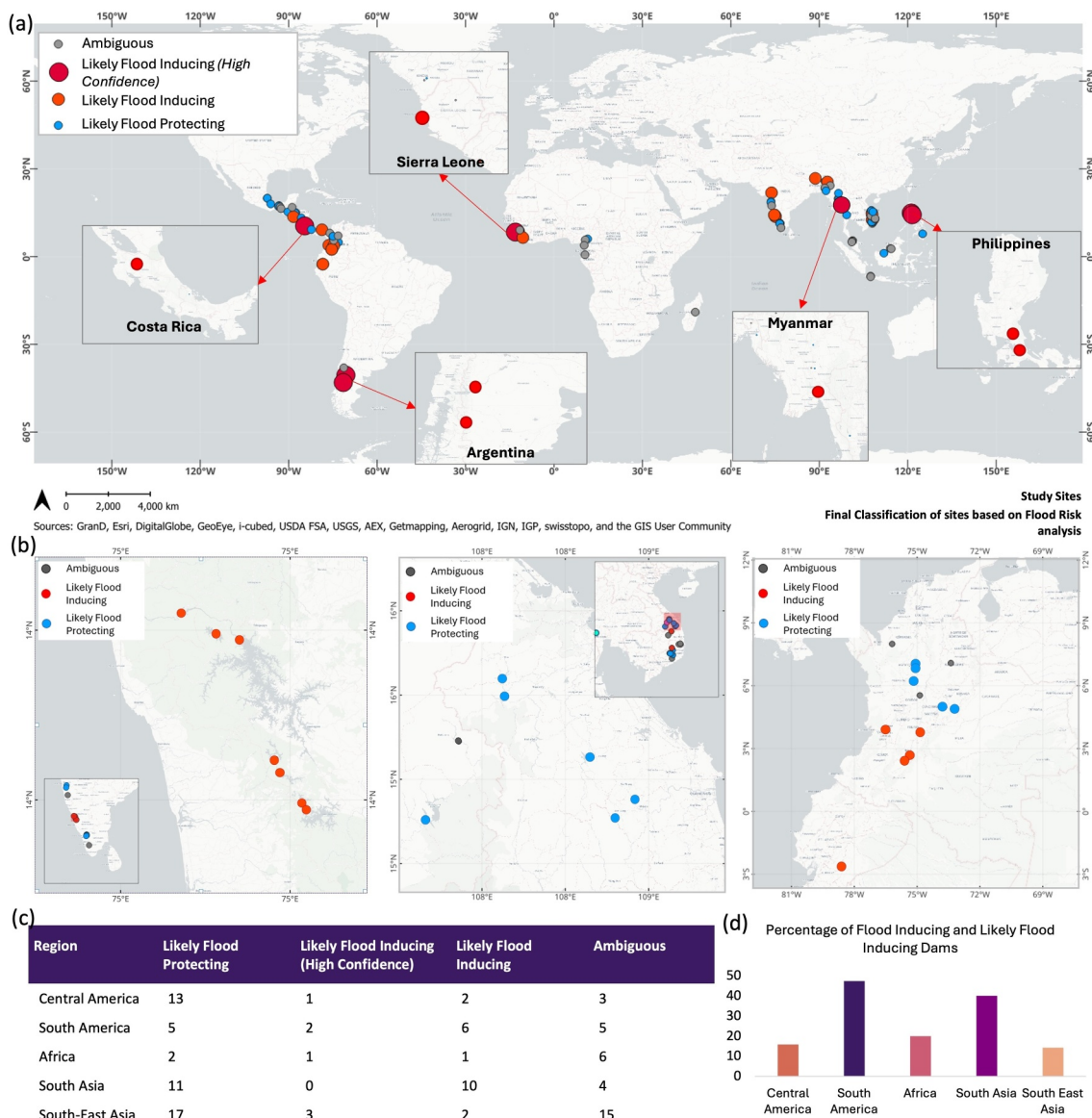


Figure 8. (a) Map with study site locations and classification labels. Location of study sites that are classified as “Likely Flood Inducing (high confidence)” are shown as inset maps. (b) Clustering of similarly classified sites within the same geographic region. (c) Table with region wise split of classifications. (d) Region wise percentage of Likely Flood Inducing (high confidence) or Likely Flood Inducing study sites.

significant difference between correlation values during wet and dry periods and had a positive correlation (see Figure S5 in Supporting Information S1). This discrepancy suggests that during periods of high precipitation, reservoir outflows make a substantial additional contribution to the downstream inundated water area. Consequently, these sites were confirmed as “Likely Flood Inducing” (high confidence), indicating that reservoir outflows (and hence operations) were a primary factor driving increased downstream inundation during wet periods. The final classification is shown in Figure 7c.

The global distribution of study sites, classified based on initial and confirmatory flood risk analyses, is presented in Figure 8. This distribution reveals notable regional variability, with South America and South Asia exhibiting a higher concentration of “Likely Flood Inducing” and “Likely Flood Inducing (high confidence)” sites. South America has the highest proportion of dams classified as such, accounting for 47.4% of studied sites, reflecting significant downstream flood risks in this region. In contrast, South-East Asia has the highest number of dams classified as “Likely Flood Protecting,” representing 45.9% of its total sites, indicative of more effective reservoir management practices or favorable hydrological conditions in these areas.

Maps in the inset in Figure 8a emphasize specific regions such as Sierra Leone, Costa Rica, Argentina, Myanmar, and the Philippines, where flood-inducing classifications are particularly prominent. Figure 8b shows specific regions of interest, such as southwestern India and Vietnam illustrating the spatial clustering of study sites. Sites with similar classifications are found to be located in close proximity, reinforcing the idea that regional reservoir management practices and hydrological regimes strongly influence classification outcomes. Such clustering suggests that local operational strategies based on static rule curves and compounded with similar hydroclimatic trends could contribute to the higher prevalence of flood-inducing sites in these regions.

Overall, the spatial patterns observed emphasize the need for region-specific approaches to hydropower and flood risk management, that accounts for the interplay between hydrological variability, reservoir operations, and downstream impacts.

5. Discussions

The results elucidated from our comprehensive multi-decadal and data-driven study indicate an intricate and nuanced relationship between reservoir operations, regional hydrological variability, and downstream flood risk. As mentioned earlier, the absence of extensive pre-dam data required the use of control sites to act as a proxy for regions with similar characteristics as the selected hydropower dams but without the influence of any upstream water storage facilities. These control sites added rigor to our analysis of the effect of hydropower dams on downstream flooding. The integration of flood intensity and frequency into a combined test score added a multidimensional perspective to the analysis. This approach ensured that both the severity (intensity) and likelihood (frequency) of potential flooding were considered while classifying the sites.

The initial classification showed that while 41.1% of study sites were categorized as Likely Flood Protecting, a significant 26.2% exhibited Likely Flood Inducing characteristics, prompting further analysis. The confirmatory phase, using multi-decadal modeled outflows from RAT 3.0, identified dams where operations appear to exacerbate downstream flooding. Exceedance probability curves and correlation-based assessments revealed heightened vulnerability at these sites, particularly during extreme precipitation events. Geospatial analysis indicated regional clustering of Likely Flood Inducing dams, highlighting the role of local operational strategies and hydro-climatic factors, such as rising precipitation in influencing flood outcomes. Regions like South America and South Asia emerged as hotspots for flood risk, while Southeast Asia showed more protective outcomes, which may reflect region-specific reservoir design or operational practices. However, this interpretation is based on spatial patterns in our analysis and warrants further investigation. Thus, these findings underscore the need for region-specific and flexible operational strategies to effectively balance downstream flood mitigation with sustainable hydropower production.

A comprehensive understanding of the nuanced differences observed between the classified sites (Likely Flood Inducing vs. Likely Flood Protecting) can be achieved by looking at several key variables such as urbanization growth and energy demand changes, precipitation patterns, reservoir characteristics, and land cover changes. Since the sites that were classified as “Likely Flood Inducing” with a high degree of confidence are very less (6% of sites), they have been clubbed together with “Likely Flood Inducing” sites for the following analysis. Figure 9 and Table 2 showcase the distribution of values for 10 geoclimatic variables across sites classified as “Likely Flood Inducing” and “Likely Flood Protecting.”

With respect to precipitation, “Likely Flood Inducing” sites are found to experience 34% higher mean annual precipitation and a 70% higher annual precipitation growth rate compared to “Likely Flood Protecting” sites. This indicates that “Likely Flood Inducing” sites are exposed to more intense and rapidly increasing precipitation regimes, which can lead to elevated risks of flooding if water management systems are inadequate. The higher growth rate of precipitation suggests that these areas are more susceptible to climate change, potentially overwhelming existing hydrological infrastructure. In contrast, “Likely Flood Protecting” sites may benefit from either lower climatic pressures or better-designed systems that effectively moderate precipitation impacts.

Reservoir characteristics, particularly the annual surface area growth rate, reveal that flood-inducing sites exhibit a more pronounced negative surface area growth ($-0.07 \text{ km}^2/\text{year}$) compared to flood-protecting sites ($-0.02 \text{ km}^2/\text{year}$). This trend may reflect sedimentation or reservoir shrinkage, which diminishes storage capacity and exacerbates downstream flood risks by reducing the reservoir's ability to buffer excess inflows. Figure S6 in Supporting Information S1 provides additional context, displaying the locations of “Likely Flood Inducing (high

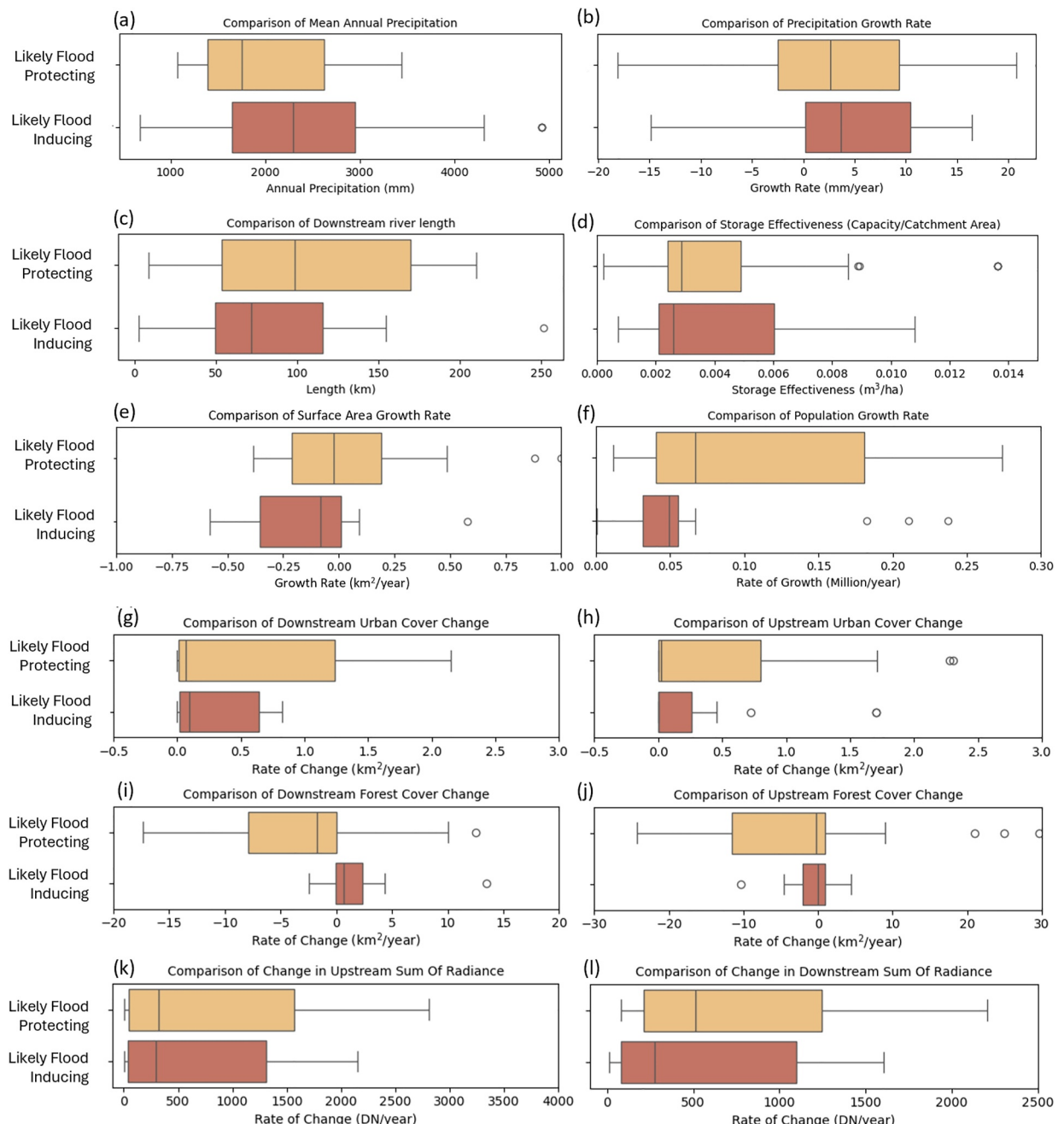


Figure 9. Box plots of key geographical and climatological variables for “Likely Flood Inducing” and “Likely Flood Protecting” sites. (a) Mean annual precipitation. (b) Annual precipitation growth rate. (c) Downstream river length. (d) Storage effectiveness ratio (Reservoir capacity/Catchment area). (e) Reservoir surface area growth rate. (f) Population growth rate (around 100 km radius of study site). (g, h) Downstream and upstream yearly urban cover (i, j) Downstream and upstream yearly forest cover change; Nightlight data: (k, l) yearly change in downstream and upstream sum of light radiance. A complementary classification-first summary is provided in Table S3 in Supporting Information S1.

confidence) and “Likely Flood Inducing” sites overlaid on a heatmap of reservoir capacity loss rates derived from the Global Reservoir Inventory of Lost Storage by Sedimentation (GRILSS v1.1) data set (Minocha & Hossain, 2025). Notably, many of the sites identified as at risk of flooding are situated in regions with high sedimentation-induced capacity loss rates. This spatial correlation underscores the critical role of sedimentation management in mitigating flood risks and highlights the importance of prioritizing maintenance and rehabilitation efforts in sediment-prone regions to sustain reservoir performance and flood protection.

Table 2
Median Values for Geographic and Climatological Variables for Classified Study Sites

Classification variable	Likely flood protecting	Likely flood inducing
Precipitation		
Mean precipitation	1833.1 mm	2461.7 mm
Annual precipitation growth rate	3.3 mm/year	5.6 mm/year
Reservoir characteristics		
Annual surface area growth rate	-0.023 km ² /year	-0.074 km ² /year
Storage effectiveness ratio	0.0028 m ³ /ha	0.0029 m ³ /ha
Downstream river length	85.1 km	54.6 km
Population and land cover		
Population growth rate	0.067 M/year	0.049 M/year
Downstream yearly urban cover change	0.07 km ² /year	0.1 km ² /year
Upstream yearly urban cover change	0.02 km ² /year	0.003 km ² /year
Downstream yearly forest cover change	-1.8 km ² /year	0.64 km ² /year
Upstream yearly forest cover change	-0.25 km ² /year	-0.02 km ² /year
Nightlight		
Downstream yearly change in sum of radiance	510.6 DN/year	272.4 DN/year
Upstream yearly change in sum of radiance	318 DN/year	300 DN/year

The storage effectiveness, defined as the ratio of reservoir capacity to catchment area, is nearly identical for both classifications, averaging around 0.003 m³/ha. These values are characteristic of hydropower and multipurpose reservoirs (based on the GranD reservoir database), which typically feature extensive catchment areas relative to their volumetric storage capacities.

Interestingly, the downstream river length or length of influence region of “Likely Flood Protecting” sites is significantly longer, with a median value that is 56% greater than the “Likely Flood Inducing” sites. This longer downstream river length likely plays a critical role in mitigating flood risks by providing more channel storage to distribute the excess water, thereby reducing the potential for localized inundation. It may also contribute to more gradual water flow and enhanced opportunities for natural infiltration and sediment deposition, which help buffer against sudden surges in water levels. In contrast, the relatively shorter downstream river lengths observed in flood-inducing sites limit the capacity for longitudinal water dispersal, increasing the likelihood of intense flooding events across the riverbanks in these regions.

Population growth, urbanization, and land cover change patterns show contrasting trends between Likely Flood Inducing and Likely Flood Protecting hydropower dam sites. Population growth rates at flood-inducing sites are 29% lower, suggesting that flood-protecting dams are located in more urbanized and economically active areas. These sites also saw greater increases in urban cover and nighttime light intensity, indicating infrastructure expansion and higher socio-economic activity, likely driven by the perceived safety and stability offered by well-managed dams.

Land cover trends similarly diverge. Flood-protecting sites experienced more forest loss upstream and downstream, likely due to increased development pressure, while flood-inducing sites saw less deforestation, reflecting lower population density and economic activity. These findings suggest that forest loss alone is not a reliable indicator of downstream flood risk, and must be interpreted alongside socio-economic context. The concentration of development near flood-protecting dams underscores their role in attracting population inflows and driving economic growth, but also highlights trade-offs such as long-term environmental degradation through deforestation and land use change.

The robustness of the median-difference patterns shown in Figure 9 was looked at further by repeating the analysis using a classification-first approach (Table S3 in Supporting Information S1). Study sites were grouped into low, medium, and high classes for six hydro-climatic and socio-economic variables, along with an aggregated

Köppen-Geiger climate zone (Beck et al., 2023). Within each class, the proportion of dams classified as likely flood-inducing or flood-protecting was tallied. This alternative framing produced results consistent with the main analysis. Temperate climates and long downstream reaches contained a larger share of likely flood protecting sites, whereas high precipitation-growth and net reservoir-area loss bins exhibited elevated likely flood-inducing fractions. These patterns strengthen the inference that climatic regime, storage dynamics, and reach length jointly modulate downstream flood behavior.

6. Conclusions

Hydropower dams are the lifeline of many communities across the world, particularly in developing regions of the world. They remain a cornerstone of global efforts to meet growing energy demands amidst net-zero carbon targets by providing cheap, reliable, renewable, and around-the-clock energy. This study reveals an intricate balance between the dual roles of hydropower dams in renewable energy production and flood risk management, under fast-changing geoclimatic conditions.

In answering the question posed earlier (*Has hydropower made the world more flood-prone?*) our study revealed nuanced results. A significant portion of the analyzed dam sites demonstrated the ability to mitigate downstream flood risks to a large extent, likely benefiting from stringent design of dams for flood safety, localized and adaptive operational strategies, longer downstream river lengths, or favorable hydro-climatic trends. However, about 26.2% of hydropower dams were found to likely exacerbate downstream flooding risks, with around 6% of reservoirs found to have a significant detrimental impact on flooding situation with a high degree of confidence. This is primarily due to disparities in mean annual precipitation, greater growth and variability in precipitation rates, and the occurrence of extreme precipitation events. Additionally, such dam sites exacerbated downstream flood risk for shorter downstream river lengths. These sites also experience significant loss of storage capacity due to sedimentation and are often located in less urbanized areas.

As the world continues to build more hydropower facilities than ever before, it is critical to examine and update current operational guidelines and planning policies. The use of operational procedures based on pre-dam data (called static rule curves) must be re-evaluated in favor of dynamic forecast-informed reservoir operations (FIRO) (Bertoni et al., 2021; Das, Suresh, et al., 2024). The economic benefits and improvements to flood moderation capabilities of using FIRO in the context of maximizing hydropower generation have been proven in many past studies (such as by Ahmad and Hossain (2019)).

Policies must be updated and modernized by incorporating broader guidelines for existing and future hydropower facilities. For new dams, expansion should prioritize regions where hydropower can provide maximum benefits while being located in a hydro-climatologically stable region with sufficient downstream river reach length. There needs to be sufficient downstream reach and floodplain area to absorb flood waters released by dams. High sedimentation rates reduce reservoir capacity and critically the flood buffer, exacerbating flood risks and diminishing energy production efficiency. Regular dredging and the adoption of sediment bypass systems should become integral components of dam management strategies.

Dams currently categorized as “Likely Flood Protecting” may evolve over time to become potentially “Likely Flood Inducing” if not managed adaptively under evolving climatic and hydrological conditions. There is a lesson to be learned for the currently classified “Likely Flood Protecting” hydropower dams from the culprit factors of “Likely Flood Inducing” ones to avoid the potential fate of exacerbating downstream floods in future. As environmental and operational dynamics shift, even these seemingly protective structures could exacerbate downstream flooding without proactive measures if the gradual change in hydro-climatology, storage capacity reduction and reduction in downstream river length are not taken into account. Any intervention should be informed by thorough and updated assessments of flood risks as conducted in this study, leveraging high-resolution precipitation models, advanced climate projections, and hydrological analyses to ensure infrastructure resilience against extreme events.

While this study provides valuable insights into the dual roles of hydropower dams in energy production and flood risk management, several limitations warrant consideration. First, the reliance on satellite-derived data sets, while comprehensive and possibly the only way to perform global analyses, introduces potential inaccuracies, particularly in regions with persistent cloud cover or limited data resolution. These limitations may affect the precision of reservoir storage and outflow estimates.

Second, the use of control sites to infer pre-dam flood conditions is inherently constrained by the assumption of similarity between study and control regions, which may not completely account for unique hydrological or climatic nuances. Although we implemented a slope-aware, multi-criteria matching framework, it may not fully capture site-specific hydrologic or geomorphic features. Particularly, in rare instances where the extent of flat, flood-prone terrain is significantly larger in either the study or control ROI, it may result in exaggerated flood signals simply due to greater opportunity for floodwaters to spread. This discrepancy could lead to misclassification of a dam's flood influence, despite the use of normalized water area metrics. Finally, the absence of extensive data on sedimentation rates, reservoir maintenance practices, and transboundary water management is another aspect that requires consideration.

Ultimately, the future of hydropower must involve a holistic approach that addresses its dual roles in energy production and flood control. By combining robust policy frameworks, technological innovations, and interdisciplinary research, the sustainable management of hydropower dams can be achieved, ensuring they continue to benefit communities and help in achieving emission targets, while minimizing flood risks to downstream regions and ecosystems.

Data Availability Statement

Study site and control site geospatial data are made available in Suresh and Hossain (2025a). All other data sets used in the study are freely accessible.

Python code used to download data sets, generate subsequent data and results seen in the manuscript are made available in Suresh and Hossain (2025b).

The RAT 3.0 software code is available in Minocha, Das, Suresh, and Hossain (2025).

Acknowledgments

This study was supported by a NASA grant from the Earth Science Action program in Water Resources 80NSSC22K0918.

Additional support from the NASA Physical Oceanography Program (80NSSC24K1644) is also gratefully acknowledged.

References

- Abass, K., Dumedad, G., & Frempong, F. (2022). Understanding the physical and human contexts of fluvial floods in rural Ghana. *International Journal of River Basin Management*, 20(2), 141–152. <https://doi.org/10.1080/15715124.2019.1653310>
- Ahmad, S. K., & Hossain, F. (2019). A generic data-driven technique for forecasting of reservoir inflow: Application for hydropower maximization. *Environmental Modelling & Software*, 119, 147–165. <https://doi.org/10.1016/j.envsoft.2019.06.008>
- Ahmad, S. K., & Hossain, F. (2020). Forecast-informed hydropower optimization at long and short-time scales for a multiple dam network. *Journal of Renewable and Sustainable Energy*, 12(1), 014501. <https://doi.org/10.1063/1.5124097>
- Alexander, L. V., Zhang, X., Peterson, T. C., Caesar, J., Gleason, B., Klein Tank, A. M. G., et al. (2006). Global observed changes in daily climate extremes of temperature and precipitation. *Journal of Geophysical Research*, 111(D5). <https://doi.org/10.1029/2005JD006290>
- Beck, H. E., McVicar, T. R., Vergopolan, N., Berg, A., Lutsko, N. J., Dufour, A., et al. (2023). High-resolution(1 km) Köppen-Geiger maps for 1901–2099 based on constrained CMIP6 projections. *Scientific Data*, 10(1), 724. <https://doi.org/10.1038/s41597-023-02549-6>
- Bennett, A. R., Hamman, J. J., & Nijssen, B. (2020). MetSim: A Python package for estimation and disaggregation of meteorological data. *Journal of Open Source Software*, 5(47), 2042. <https://doi.org/10.21105/joss.02042>
- Bertoni, F., Giuliani, M., Castelletti, A., & Reed, P. M. (2021). Designing with information feedbacks: Forecast informed reservoir sizing and operation. *Water Resources Research*, 57(3), e2020WR028112. <https://doi.org/10.1029/2020WR028112>
- Biswas, N. K., Hossain, F., Bonnema, M., Lee, H., & Chishtie, F. (2021). Towards a global reservoir assessment tool for predicting hydrologic impacts and operating patterns of existing and planned reservoirs. *Environmental Modelling & Software*, 140, 105043. <https://doi.org/10.1016/j.envsoft.2021.105043>
- Bonnema, M., & Hossain, F. (2017). Inferring reservoir operating patterns across the Mekong Basin using only space observations. *Water Resources Research*, 53(5), 3791–3810. <https://doi.org/10.1002/2016WR019978>
- Bonnema, M., & Hossain, F. (2019). Assessing the potential of the surface water and ocean topography mission for reservoir monitoring in the Mekong River Basin. *Water Resources Research*, 55(1), 444–461. <https://doi.org/10.1029/2018WR023743>
- Bonnema, M., Sikder, S., Miao, Y., Chen, X., Hossain, F., Ara Pervin, I., et al. (2016). Understanding satellite-based monthly-to-seasonal reservoir outflow estimation as a function of hydrologic controls. *Water Resources Research*, 52(5), 4095–4115. <https://doi.org/10.1002/2015WR017830>
- Chen, T., Song, C., Luo, S., Ke, L., Liu, K., & Zhu, J. (2022). Monitoring global reservoirs using ICESat-2: Assessment on spatial coverage and application potential. *Journal of Hydrology*, 604, 127257. <https://doi.org/10.1016/J.JHYDROL.2021.127257>
- Cooley, S. W., Ryan, J. C., & Smith, L. C. (2021). Human alteration of global surface water storage variability. *Nature*, 91(7848), 78–81. <https://doi.org/10.1038/s41586-021-03262-3>
- Das, P., Hossain, F., Khan, S., Biswas, N. K., Lee, H., Piman, T., et al. (2022). Reservoir assessment tool 2.0: Stakeholder driven improvements to satellite remote sensing based reservoir monitoring. *Environmental Modelling & Software*, 157, 105533. <https://doi.org/10.1016/j.envsoft.2022.105533>
- Das, P., Hossain, F., Minocha, S., Suresh, S., Darkwah, G. K., Lee, H., et al. (2024). ResORR: A globally scalable and satellite data-driven algorithm for river flow regulation due to reservoir operations. *Environmental Modelling & Software*, 176, 106026. <https://doi.org/10.1016/j.envsoft.2024.106026>
- Das, P., Suresh, S., Hossain, F., Balakrishnan, V., Pallipadan, J. J., Lee, H., et al. (2024). Forecast informed reservoir operations within a satellite based framework for mountainous and high precipitation regions: The case of the 2018 Kerala floods. *ASCE Journal of Hydrologic Engineering*, 30(2), 05025003. <https://doi.org/10.1061/JHYEFF.HEENG-6276>
- Dunn, O. J. (1964). Multiple comparisons using rank sums. *Technometrics*, 6(3), 241–252. <https://doi.org/10.1080/00401706.1964.10490181>

- Durand, M., Barros, A., Dozier, J., Adler, R., Cooley, S., Entekhabi, D., et al. (2021). Achieving breakthroughs in global hydrologic science by unlocking the power of multisensor, multidisciplinary Earth observations. *AGU Advances*, 2(4), e2021AV000455. <https://doi.org/10.1029/2021AV000455>
- Energy Institute. (2024). Statistical review of world energy. Retrieved from <https://www.energyinst.org/statistical-review/home>
- Fan, P., Cho, M. S., Lin, Z., Ouyang, Z., Qi, J., Chen, J., & Moran, E. F. (2022). Recently constructed hydropower dams were associated with reduced economic production, population, and greenness in nearby areas. *Proceedings of the National Academy of Sciences*, 119(8), e2108038119. <https://doi.org/10.1073/pnas.2108038119>
- Fick, S. E., & Hijmans, R. J. (2017). WorldClim 2: New 1 km spatial resolution climate surfaces for global land areas. *International Journal of Climatology*, 37(12), 4302–4315. <https://doi.org/10.1002/joc.5086>
- Gale, E. L., & Saunders, M. A. (2013). The 2011 Thailand flood: Climate causes and return periods. *Weather*, 68(9), 233–237. <https://doi.org/10.1002/wea.2133>
- Gao, H. (2015). Satellite remote sensing of large lakes and reservoirs: From elevation and area to storage. *Wiley Interdisciplinary Reviews: Water*, 2(2), 147–157. <https://doi.org/10.1002/WAT2.1065>
- Hamman, J. J., Nijssen, B., Bohn, T. J., Gergel, D. R., & Mao, Y. (2018). The Variable Infiltration Capacity model version 5 (VIC-5): Infrastructure improvements for new applications and reproducibility. *Geoscientific Model Development*, 11(8), 3481–3496. <https://doi.org/10.5194/gmd-11-3481-2018>
- IEA. (2021). *Key world energy statistics 2021*. IEA. Retrieved from <https://www.iea.org/reports/key-world-energy-statistics-2021>
- International Hydropower Association (IHA). (2022). Hydropower status report 2022. Retrieved from <https://www.hydropower.org/>
- Kruskal, W. H., & Wallis, W. A. (1952). Use of ranks in one-criterion variance analysis. *Journal of the American Statistical Association*, 47(260), 583–621. <https://doi.org/10.1080/01621459.1952.10483441>
- Kumar, S., Vardhan, A. S. S., Vardhan, A. S. S., Saket, R. K., Kothari, D. P., & Eslamian, S. (2022). Hydropower and floods. In *Flood handbook* (pp. 111–142). CRC Press. <https://doi.org/10.1201/9781003262640>
- Kundu, B. S., & Mothikumar, K. E. (1995). Mapping and management of flood-affected areas through remote sensing a case study of Sirsa district, Haryana. *Journal of the Indian Society of Remote Sensing*, 23(3), 139–146. <https://doi.org/10.1007/BF02995701>
- Lehner, B., & Grill, G. (2013). Global river hydrography and network routing: Baseline data and new approaches to study the world's large river systems. *Hydrological Processes*, 27(15), 2171–2186. <https://doi.org/10.1002/hyp.9740>
- Lehner, B., Reidy Liermann, C., Revenga, C., Vörösmarty, C., Fekete, B., Crouzet, P., et al. (2011). High-resolution mapping of the world's reservoirs and dams for sustainable river-flow management. *Frontiers in Ecology and the Environment*, 9(9), 494–502. <https://doi.org/10.1890/100125>
- Li, X., Zhou, Y., Zhao, M., & Zhao, X. (2020). A harmonized global nighttime light dataset 1992–2018. *Scientific Data*, 7(1), 168. <https://doi.org/10.1038/s41597-020-0510-y>
- Lima, I. B. T., Ramos, F. M., Bambace, L. A. W., & Rosa, R. R. (2008). Methane emissions from large dams as renewable energy resources: A developing nation perspective. *Mitigation and Adaptation Strategies for Global Change*, 13(13), 193–206. <https://doi.org/10.1007/s11027-007-9086-5>
- Liu, L., Cao, X., Li, S., & Jie, N. (2024). A 31-year (1990–2020) global gridded population dataset generated by cluster analysis and statistical learning. *Scientific Data*, 11(11), 124. <https://doi.org/10.1038/s41597-024-02913-0>
- Loc, H. H., Emadzadeh, A., Park, E., Nontiansak, P., & Deo, R. C. (2023). The Great 2011 Thailand flood disaster revisited: Could it have been mitigated by different dam operations based on better weather forecasts? *Environmental Research*, 216, 114493. <https://doi.org/10.1016/j.envres.2022.114493>
- Lohmann, D., Raschke, E., Nijssen, B., & Lettenmaier, D. P. (1998). Regional scale hydrology: I. Formulation of the VIC-2L model coupled to a routing model. *Hydrological Sciences Journal*, 43(1), 131–141. <https://doi.org/10.1080/0262669809492107>
- Mann, H. B., & Whitney, D. R. (1947). On a test of whether one of two random variables is stochastically larger than the other. *The Annals of Mathematical Statistics*, 18(1), 50–60. <https://doi.org/10.1214/aoms/117730491>
- Milly, P., Wetherald, R., Dunne, K., & Delworth, T. L. (2002). Increasing risk of great floods in a changing climate. *Nature*, 415(6871), 514–517. <https://doi.org/10.1038/415514a>
- Minocha, S., Das, P., & Hossain, F. (2025). Reservoir assessment tool (RAT): A Python package for monitoring the dynamic state of reservoirs and analyzing dam operations. *Digital Water*, 3(1), 1–30. <https://doi.org/10.1080/28375807.2025.2487762>
- Minocha, S., Das, P., Suresh, S., & Hossain, F. (2025). UW-SASWE/RAT: RAT v3.0.17 [Software]. Zenodo. <https://doi.org/10.5281/zenodo.15496137>
- Minocha, S., & Hossain, F. (2025). GRILSS: Opening the gateway to global reservoir sedimentation data curation. *Earth System Science Data*, 17(4), 1743–1759. <https://doi.org/10.5194/essd-17-1743-2025>
- Minocha, S., Hossain, F., Das, P., Suresh, S., Khan, S., Darkwah, G., et al. (2024). Reservoir assessment tool version 3.0: A scalable and user-friendly software platform to mobilize the global water management community. *Geoscientific Model Development*, 17, 3137–3156. <https://doi.org/10.5194/gmd-2023-130>
- Morris, G. L., & Fan, J. (1998). *Reservoir sedimentation handbook*. McGraw-Hill Book Co. Retrieved from <https://www.reservoirsedimentation.com/>
- Otsu, N. (1979). Threshold selection method from gray-level histograms. *IEEE Transaction on Systems, Man, and Cybernetics*, 9(1), 62–66. <https://doi.org/10.1109/TSMC.1979.4310076>
- Pekel, J. F., Cottam, A., Gorelick, N., & Belward, A. S. (2016). Global surface water–data access. *Nature*, 540(7633), 418–422. <https://doi.org/10.1038/NATURE20584>
- Penman, H. L. (1948). Natural evaporation from open water, bare soil and grass. *Proceedings of the Royal Society of London*, 193(1032), 120–145. <https://doi.org/10.1098/rspa.1948.0037>
- Poaponsakorn, N., Meethom, P., & Pantakua, K. (2014). The impact of the 2011 floods, and flood management on Thai households. In *Resilience and recovery in Asian disasters: Community ties, market mechanisms, and governance* (pp. 75–104). Springer. https://doi.org/10.1007/978-4-431-55022-8_5
- Pramanick, N., Acharyya, R., Mukherjee, S., Mukherjee, S., Pal, I., Mitra, D., & Mukhopadhyay, A. (2022). SAR based flood risk analysis: A case study Kerala flood 2018. *Advances in Space Research*, 69(4), 1915–1929. <https://doi.org/10.1016/j.asr.2021.07.003>
- Sheffield, J., Wood, E. F., Pan, M., Beck, H., Coccia, G., Serrat-Capdevila, A., & Verbist, K. J. W. R. R. (2018). Satellite remote sensing for water resources management: Potential for supporting sustainable development in data-poor regions. *Water Resources Research*, 54(12), 9724–9758. <https://doi.org/10.1029/2017WR022437>
- Snettlage, M. A., Geschke, J., Spehn, E. M., Ranipeta, A., Yoccoz, N. G., Körner, C., et al. (2022). A hierarchical inventory of the world's mountains for global comparative mountain science. *Nature Scientific Data*, 9(1), 149. <https://doi.org/10.1038/s41597-022-01256-y>

- Sudheer, K. P., Bhallamudi, S. M., Narasimhan, B., Thomas, J., Bindhu, V. M., Vema, V., & Kurian, C. (2019). Role of dams on the floods of August 2018 in Periyar River Basin, Kerala. *Current Science*, 116(5), 780–794. <https://doi.org/10.18520/cs/v116/i5/780-794>
- Suresh, S., & Hossain, F. (2025a). Hydropower and flood risk—study site and control site data (v.1.0.0) [Dataset]. Zenodo. <https://doi.org/10.5281/zenodo.15497113>
- Suresh, S., & Hossain, F. (2025b). Hydropower and flood risk GitHub repository—SarahUW/hydropower-and-flood-risk: Version 1 (v.1.0.0) [Code]. Zenodo. <https://doi.org/10.5281/zenodo.15496469>
- Suresh, S., Hossain, F., Minocha, S., Das, P., Khan, S., Lee, H., et al. (2024). Satellite-based tracking of reservoir operations for flood management during the 2018 extreme weather event in Kerala, India. *Remote Sensing of Environment*, 307, 114149. <https://doi.org/10.1016/j.rse.2024.114149>
- United Nations Framework Convention on Climate Change (UNFCCC). (2021). Glasgow Climate Pact: Decisions adopted by COP26. Retrieved from <https://unfccc.int/process-and-meetings/the-paris-agreement/the-glasgow-climate-pact-key-outcomes-from-cop26>
- Willis, A. D., Lund, J. R., Townsley, E. S., & Faber, B. A. (2011). Climate change and flood operations in the Sacramento Basin, California. *San Francisco Estuary and Watershed Science*, 9(2). <https://doi.org/10.15447/sews.2011v9iss2art3>
- Zhang, S., Gao, H., & Naz, B. S. (2014). Monitoring reservoir storage in South Asia from multisatellite remote sensing. *Water Resources Research*, 50(11), 8927–8943. <https://doi.org/10.1002/2014WR015829>
- Zhao, G., & Gao, H. (2018). Automatic correction of contaminated images for assessment of reservoir surface area dynamics. *Geophysical Research Letters*, 45(12), 6092–6099. <https://doi.org/10.1029/2018GL078343>
- Zhong, Y., Zhong, M., Mao, Y., & Ji, B. (2020). Evaluation of evapotranspiration for exorheic catchments of China during the GRACE era: From a water balance perspective. *Remote Sensing*, 12(3), 511. <https://doi.org/10.3390/rs12030511>